Examining the stability of thermally fissile Th and U isotopes

Bharat Kumar, S. K. Biswal, S. K. Singh and S. K. Patra[1]

[1] Institute of Physics, Bhubaneswar-751005, India
(Dated: November 3, 2015)

The properties of recently predicted thermally fissile Th and U isotopes are studied within the framework of relativistic mean field (RMF) approach using axially deformed basis. We calculated the ground, first intrinsic excited state for highly neutron-rich thorium and uranium isotopes. The possible modes of decay like α-decay and β-decay are analyzed. We found that the neutron-rich isotopes are stable against α-decay, however they are very much unstable against β-decay. The life time of these nuclei predicted to be tens of second against β-decay. If these nuclei utilize before their decay time, a lots of energy can be produced with the help of multi-fragmentation fission. Also, these nuclei have a great implication in astrophysical point of view. In some cases, we found the isomeric states with energy range from 2 to 3 MeV and three maxima in the potential energy surface of $^{228-230}$Th and $^{228-234}$U isotopes.

I. INTRODUCTION

Now-a-days uranium and thorium isotopes have attracted a great attention in nuclear physics due to the thermally fissile nature of some of its isotopes[1]. These thermally fissile materials have tremendous importance in energy production. Till date, the known thermally fissile nuclei are ^{233}U, ^{235}U and ^{239}Pu. Out of which only ^{235}U has a long life time and the only thermally fissile isotope available in nature [1]. Thus, presently it is an important area of research to look for any other thermally fissile nuclei apart from ^{233}U, ^{235}U and ^{239}Pu. Recently, Satpathy et al. [1] showed that uranium and thorium isotopes with neutron number N=154-172 have thermally fissile property. They performed a calculation with a typical example of ^{250}U that this nucleus has a low fission barrier with a significantly large barrier width, which makes it stable against the spontaneous fission. Apart from the thermally fissile nature, these nuclei also play an important role in the nucleosynthesis in the stellar evolution. As these nuclei are stable against spontaneous fission, thus the prominent decay modes may be the emission of α-, β- and *cluster*-particles from the neutron-rich thermally fissile (uranium and thorium) isotopes.

To measure the stability of these neutron-rich U and Th isotopes, we investigated the α- and β- decay properties of these nuclei. Also, we extend our calculations to estimate the binding energy, root mean square radii, quadrupole moments and other structural properties.

From last three decades, the relativistic mean field (RMF) formalism is a formidable theory in describing the finite nuclear properties throughout the periodic chart and infinite nuclear matter properties concerned with the cosmic dense object like neutron star. In the same line RMF theory is also good enough to study the clusterization [2], α-decay [3], and β-decay of nuclei. The presence of cluster in heavy nuclei like, ^{222}Ra, ^{232}U, ^{239}Pu and ^{242}Cm has been studied using RMF formalism [4, 5]. It gives a clear prediction of α-like

(N=Z) matter at the central part for heavy nuclei and *cluster*-like structure (N=Z and $N \neq Z$) for light mass nuclei [2]. The proton emission as well as the cluster decay phenomena are well studied using RMF formalism with M3Y [6], LR3Y [7] and NLR3Y[8] nucleon-nucleon potentials in the framework of single and double folding models, respectively. Here, we used the relativistic mean field (RMF) formalism with the well known NL3 parameter set [9] for all our calculations.

The paper is organized as follows: The RMF formalism is outlined briefly in Section II. The importance of pairing correlation and inclusion with BCS approximation are also given in this section. The results obtained from our calculations for binding energy, basis selection, potential energy surface (PES) diagrams and the evaluation of single-particle levels are discussed in Section III. The Q_α- and Q_β-values are calculated in section IV. In this section, various decay modes are discussed using empirical formula and limitation of the model is also given same section. Finally, a brief summary and concluding remarks are given in the last Section V.

II. FORMALISM

In present manuscript, we used the axially deformed relativistic mean field formalism to calculate various nuclear phenomena. The meson-nucleon interaction is given by [10–15]

$$
\begin{aligned}
\mathscr{L} = & \; \overline{\psi_i}\{i\gamma^\mu \partial_\mu - M\}\psi_i + \frac{1}{2}\partial^\mu \sigma \partial_\mu \sigma - \frac{1}{2}m_\sigma^2 \sigma^2 \\
& - \frac{1}{3}g_2\sigma^3 - \frac{1}{4}g_3\sigma^4 - g_s\overline{\psi_i}\psi_i\sigma - \frac{1}{4}\Omega^{\mu\nu}\Omega_{\mu\nu} \\
& + \frac{1}{2}m_w^2 V^\mu V_\mu + \frac{1}{4}c_3(V_\mu V^\mu)^2 - g_w\overline{\psi_i}\gamma^\mu\psi_i V_\mu \\
& - \frac{1}{4}\vec{B}^{\mu\nu}.\vec{B}_{\mu\nu} + \frac{1}{2}m_\rho^2\vec{R}^\mu.\vec{R}_\mu - g_\rho\overline{\psi_i}\gamma^\mu\vec{\tau}\psi_i.\vec{R}^\mu \\
& - \frac{1}{4}F^{\mu\nu}F_{\mu\nu} - e\overline{\psi_i}\gamma^\mu\frac{(1-\tau_{3i})}{2}\psi_i A_\mu.
\end{aligned}
\tag{1}
$$

Where, ψ is the Dirac spinor and meson fields are denoted by σ, V^μ and R^μ for σ, ω and $\rho-$ meson respectively. The electromagnetic interaction between the proton is denoted by

---

photon field A^μ. g_s, g_ω, g_ρ and $\frac{e^2}{4\pi}$ are the coupling constants for the σ, ω and $\rho-$ meson and photon field respectively. The strength of the self coupling $\sigma-$ meson (σ^3 and σ^4) are denoted by g_2 and g_3, along with c_3 as the non-linear coupling constant for ω meson. The nucleon mass is scripted as M, where the σ, ω, and $\rho-$ meson masses are m_s, m_ω and m_ρ respectively. From the classical Euler-Lagrangian equation, we get the Dirac-equation and Klein- Gordan equation for the nucleon and meson field respectively. The Dirac-equation for the nucleon is solved by expanding the Dirac spinor into lower and upper component, while the mean field equation for the Bosons are solved in deformed harmonic oscillator basis with β_0 as the deformation parameter. The nucleon equation along with different meson equation form a coupled set of equation, which can be solved by iterative method. Various types of densities such as baryon (vector), scalar, isovector and proton (charge) densities are given as

$$\rho(r) = \sum_i \psi_i^\dagger(r)\psi_i(r), \tag{2}$$

$$\rho_s(r) = \sum_i \psi_i^\dagger(r)\gamma_0\psi_i(r), \tag{3}$$

$$\rho_3(r) = \sum_i \psi_i^\dagger(r)\tau_3\psi_i(r), \tag{4}$$

$$\rho_p(r) = \sum_i \psi_i^\dagger(r)\left(\frac{1-\tau_3}{2}\right)\psi_i(r). \tag{5}$$

The calculations are simplified under the shadow of various symmetries like conservation of parity, no-sea approximation and time reversal symmetry, which kills all spatial components of the meson fields and the anti-particle states contribution to nuclear observable. The center of mass correction is calculated with the non-relativistic approximation, which gives $E_{c.m} = \frac{3}{4}41A^{-1/3}$ (in MeV). The quadrupole deformation parameter β_2 is calculated from the resulting quadropole moments of the proton and neutron. The binding energy and charge radius are given by well known relation [16–18].

A. Pairing correlations in RMF formalism

In nuclear structure physics, the pairing correlation has an indispensable role in open shell nuclei. The priority of the pairing correlation escalates with mass number A. It also plays a crucial role for the understanding of deformation of heavy nuclei. Because of the limited pair near the Fermi surface, it has a nominal effect for light mass nuclei on both bulk and single-particle properties. In the present case, we consider only T=1 channel of pairing correlation, i.e., pairing between proton-proton and neutron-neutron. In such case, a nucleon of quantum state $|j, m_z\rangle$ pairs with another nucleon having same I_z value with quantum state $|j, -m_z\rangle$, which is the time reversal partner of other. The philosophy of BCS pairing is same both in nuclear and atomic domain. The first evidence of the pairing energy came from the even-odd mass staggering of isotopes. In mean field formalism the violation of par-

ticle number is account of pairing correlation. The RMF Lagrangian density only accommodates term like $\psi^\dagger\psi$ (density) and no term of the form $\psi^\dagger\psi^\dagger$ or $\psi\psi$. The inclusion of pairing correlation of the form $\psi\psi$ or $\psi^\dagger\psi^\dagger$ violates the particle number conservation [19]. Thus, a constant gap BCS-type simple prescription is adopted in our calculations to take care of the pairing correlation for open shell nuclei. The general expression for pairing interaction to the total energy in terms of occupation probabilities v_i^2 and $u_i^2 = 1 - v_i^2$ is written as [19, 20]:

$$E_{pair} = -G\left[\sum_{i>0} u_i v_i\right]^2, \tag{6}$$

with G = pairing force constant. The variational approach with respect to the occupation number v_i^2 gives the BCS equation [20]:

$$2\varepsilon_i u_i v_i - \triangle(u_i^2 - v_i^2) = 0, \tag{7}$$

with $\triangle = G\sum_{i>0} u_i v_i$.

The densities with occupation number is defined as:

$$n_i = v_i^2 = \frac{1}{2}\left[1 - \frac{\varepsilon_i - \lambda}{\sqrt{(\varepsilon_i - \lambda)^2 + \triangle^2}}\right]. \tag{8}$$

For the pairing gap ($\triangle$) of proton and neutron is taken from the phenomenological formula of Madland and Nix [21]:

$$\triangle_n = \frac{r}{N^{1/3}}exp(-sI - tI^2) \tag{9}$$

$$\triangle_p = \frac{r}{Z^{1/3}}exp(sI - tI^2) \tag{10}$$

where, $I = (N-Z)/A$, $r = 5.73$ MeV, $s = 0.117$, and $t = 7.96$.

The chemical potentials λ_n and λ_p are determined by the particle numbers for neutrons and protons. The pairing energy of the nucleons using equation (7) and (8) can be written as:

$$E_{pair} = -\triangle\sum_{i>0} u_i v_i. \tag{11}$$

In constant pairing gap calculation, for a particular value of pairing gap $\triangle$ and force constant G, the pairing energy E_{pair} diverges, if it is extended to an infinite configuration space. In fact, in all realistic calculations with finite range forces, the contribution of states of large momenta above the Fermi surface (for a particular nucleus) to $\triangle$ decreases with energy. Therefore, the pairing window in all the equations are extended upto the level $|\varepsilon_i - \lambda| \leq 2(41A^{-1/3})$ as a function of the single particle energy. The factor 2 has been determined so as to reproduce the pairing correlation energy for neutrons in ^{118}Sn using Gogny force [18, 19, 22]. We notice that recently Karatzikos et al. [23] has been shown that if it is adjusted a constant pairing window for a particular deformation then it may leads to errors at different energy solution (different state solution). However, this kind of approach have not taken into account in our calculations, as we have adjusted to reproduce the pairing as a whole for ^{118}Sn nucleus.

It is a tough task to compute the binding energy and quadrupole moment of odd-N or odd-Z or both N and Z numbers are odd (odd-even, even-odd, or odd-odd) nuclei. To do

this, one needs to include the additional time-odd term, as is done in the SHF Hamiltonian [24], or empirically the pairing force in order to take care the effect of odd-neutron or odd-proton [25]. In an odd-even or odd-odd nucleus, the time reversal symmetry gets violated in the mean field models. In our RMF calculations, we neglect the space components of the vector fields, which are odd under time reversal and parity. These are important in the determination of magnetic moments [26] but have a very small effects on bulk properties such as binding energies or quadrupole deformations, and they can be neglected[27] in the present context. Here, for the odd-Z or odd-N calculations, we employ the Pauli blocking approximation, which restores the time-reversal symmetry. In this approach, one pair of conjugate states, $\pm m$, is taken out of the pairing scheme. The odd particle stays in one of these states, and its corresponding conjugate state remains empty. In principle, one has to block in turn different states around the Fermi level to find the one that gives the lowest energy configuration of the odd nucleus. For odd-odd nuclei, one needs to block both the odd neutron and odd proton.

III. CALCULATIONS AND RESULTS

In this Section, we evaluate our results for binding energy, rms radii, quadrupole deformation parameter for recently predicted thermally fissile isotopes of Th and U. These nuclei are quite heavy and needed a large number of oscillator basis, which takes considerable time for computation. We spent few lines in the first subsection of this section to describe how to select basis space and the results and discussions are followed subsequently.

A. Selection of basis space

The Dirac equation for Fermions (proton and neutron) and the equation of motion for Bosons ($\sigma-$, $\omega-$, $\rho-$ and A_0) obtained from the RMF Lagrangian are solved self-consistently using an iterative methods. These equations are solved in an axially deformed harmonic oscillator expansion basis N_F and N_B for Fermionic and Bosonic wavefunction, respectively.

For heavy nuclei, a large number of basis space N_F and N_B are needed to get a converged solution. To reduce the computational time without compromising the convergence of the solution, we have to choose an optimal number of model space for both Fermion and Boson fields. To choose optimal values for N_F and N_B, we select ^{240}Th as a test case and increase the basis quanta from 8 to 20 step by step. The obtained results of binding energy, charge radii and quadrupole deformation parameter are shown in Fig. 1. From our calculations, we notice an increment of 200 MeV in binding energy while going from $N_F = N_B =8$ to 10. This increment in energy decreases while going to higher oscillator basis. For example, change in energy is ~ 0.2 MeV with a change of $N_F = N_B$ from 14 to 20 and the increment in r_c values are 0.12 fm respectively. Keeping in mind the increase in convergence time for larger quanta as well as the size of the nuclei considered, we have

finalized to use $N_F = N_B = 20$ in our calculations to get a suitable convergent results, which is the current accuracy of the present RMF models.
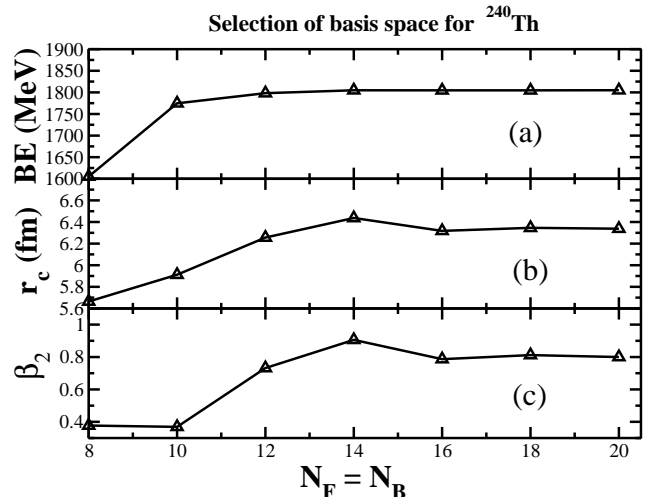

FIG. 1: The variation of calculated binding energy (BE), charge radii (r_c) and quadrupole deformation parameter (β_2) are given with Bosonic and Fermionic basis.

B. Binding energies, charge radii and quadrupole deformation parameters

To be sure about the predictivity of our model, first of all we calculate the binding energies (BE), charge radii r_c and quadrupole deformation parameter β_2 for some of the known cases. We have compared our results with the experimental data wherever available or with the Finite Range Droplet Model (FRDM) of Möller et al. [28–31]. The results are displayed in Tables I and II. From the tables, it is obvious that the calculated binding energies are comparable with the FRDM as well as experimental values. A further inspection of the tables reveal that the FRDM results are more closer to the data. This may be due to the fitting of the FRDM parameters for almost all known data. However, in case of most RMF parametrizations, the constants are determined by using few spherical nuclei data along with certain nuclear matter properties. Thus the prediction of the RMF results are considered to be reasonable, but not excellent.

Ren et al. [32, 33] have reported that the ground state of several superheavy nuclei are highly deformed states. Since, these are very heavy isotopes, the general assumption is that the ground state most probably remains in deformed configuration (liquid drop picture). When these nuclei excited either by a thermal neutron or by any other means, it's intrinsic excited state becomes extra-ordinarily deformed and attains the scission point before it goes to fission. This can also be easily realized from the potential energy surface (PES) curve. Our calculations agree with the prediction of Ren et al. for other

superheavy region of the mass table. However, this conclusion is contradicted by [34]. According to him, the ground state of superheavy nuclei either spherical or normally deformed.

In some cases of U and Th isotopes, we get more than one solution. The solution corresponding to the maximum binding energy is the ground state configuration and all other solutions are the intrinsic excited states. In some cases, the ground state binding energy does not match with the experimental data. However, the binding energy, whose quadrupole deformation parameter β_2 is closer to the experimental data or to the FRDM value matches well with each other. For example, binding energies of ^{236}U are 1791.7, 1790.0 and 1790.4 MeV with RMF, FRDM and experimental data, respectively and the corresponding β_2 are 0.276, 0.215 and 0.272. Similar to the binding energy, we get comparable β_2 and charge radius r_c of RMF results with the FRDM and experimental values.

C. Potential energy surface (PES)

In late 1960's, the structure of potential energy surface (PES) has been renewed interest for it's role in nuclear fission process. In majority of PES for actinide nuclei, there exists a second maximum, which split the fission barrier into inner and outer segments [35]. It has also a crucial role for the characterization of ground state, intrinsic excited state, occurrence of the shape coexistence, radioactivity, spontaneous and induced fission. The structure of the potential energy surface is defined mainly from the shell structure which is strongly related to the distance between the mass centers of the nascent fragments. The macroscopic-microscopic liquid drop theory has been given a key concept of fission, where the surface energy is the form of collective deformation of the nucleus.

In Figs. 2 and 3 we have plotted the PES for some selected isotopes of Th and U nuclei. The constraint binding energy BE_c versus the quadrupole deformation parameter β_2 are shown. A nucleus undergoes fission process, when the nucleus becomes highly elongated along an axis. This can be done in a simplest way by modifying the single-particle potential with the help of a constraint, i.e., the Lagrangian multiplier λ. Then, the system becomes more or less compressed depending on the Lagrangian multiplier λ. In other word, in a constraint calculation, we minimize the expectation value of the Hamiltonian $< H' >$ instead of $< H >$ which are related to each other by the following relation [36–40]:

$$H' = H - \lambda Q, \qquad with \qquad Q = r^2 Y_{20}(\theta, \phi), \qquad (12)$$

where, λ is fixed by the condition $< Q >_\lambda = Q_0$.

Usually, in an axially deformed constraint calculation for a nucleus, we see two maxima in the PES diagram, (i) prolate and (ii) oblate or spherical. However, in some cases, more than two maxima are also seen. If the ground state energy is distinctly more than other maxima, then the nucleus has a well defined ground state configuration. On the other hand, if the difference in binding energy between two or three maxima is negligible, then the nucleus is in shape co-existence configuration. In such a case, a configuration mixing calculation is
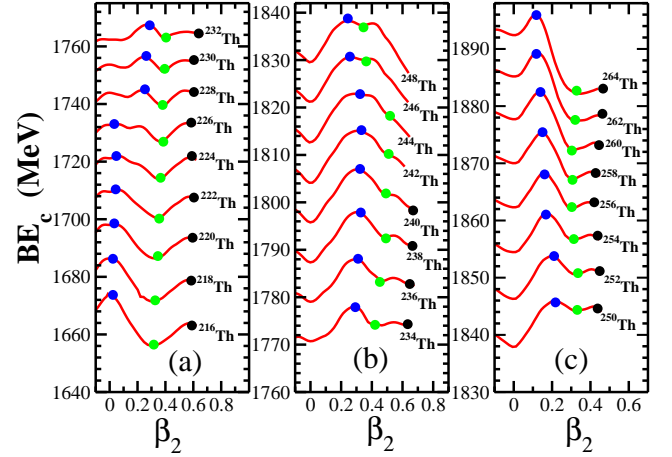

FIG. 2: (Color online) The potential energy surface is a function of quadrupole deformation parameter (β_2) for Th isotopes. The difference between blue and green dots represents first fission barrier heights B_f (in MeV). See text for details.
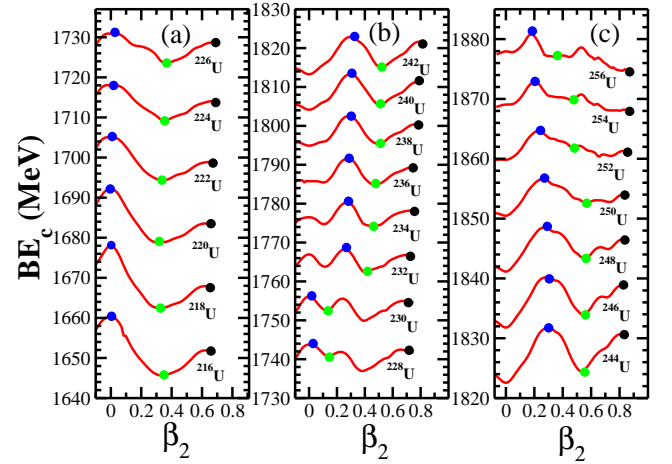

FIG. 3: (Color online) Same as Fig. 2, but for U isotopes.

needed to determine the ground state solution of the nucleus, which is beyond the scope of the present calculation. It is to be noted here that in a constraint calculation, the maximum binding energy (major peak in the PES diagram) corresponds to the ground state configuration and all other solutions (minor peaks in the PES curve) are the intrinsic excited states.

The fission barrier B_f is an important quantity to study the properties of fission reaction. We calculate the fission barrier from the PES curve for some selected even-even nuclei, which are displayed in Table III. From the table, it can be seen that the fission barrier for ^{228}Th comes out to be 5.69 MeV comparable to the FRDM and experimental values of B_f = 7.43 and

TABLE I: The calculated binding energies BE, quadrupole deformation parameter β_2, rms radii for the ground states and few selective intrinsic excited state of U isotopes, using RMF formalism with NL3 parameter set. The experimental and FRDM data [28–31] are also included in the table. See the text for more details.

| Nucleus | RMF (NL3) | | | | | | FRDM | | Experiment | | |
	r_n	r_p	r_{rms}	r_{ch}	β_2	BE (MeV)	BE(MeV)	β_2	r_{ch}	β_2	BE (MeV)
^{216}U	5.762	5.616	5.700	5.673	0	1660.5	1649.0	-0.052			
	6.054	5.946	6.008	5.999	0.608	1650.8					
^{218}U	5.789	5.625	5.721	5.682	0	1678.0	1666.7	0.008			1665.6
	6.081	5.957	6.029	6.011	0.606	1666.9					
^{220}U	5.819	5.641	5.745	5.698	0	1692.2	1681.2	0.008			1680.8
	6.109	5.971	6.052	6.025	0.605	1682.6					
^{222}U	5.849	5.661	5.772	5.717	0	1705.1	1695.7	0.048			1695.6
	6.142	5.990	6.079	6.043	0.611	1697.9					
^{224}U	5.878	5.681	5.798	5.737	0	1717.9	1710.8	0.146			1710.3
	6.198	6.032	6.131	6.085	0.645	1712.8					
^{226}U	5.907	5.701	5.824	5.757	0	1730.8	1724.7	0.172			1724.8
	6.232	6.053	6.160	6.106	0.652	1727.4					
^{228}U	5.935	5.721	5.850	5.776	0	1743.6					
	5.966	5.743	5.877	5.798	0.210	1741.7	1739.0	0.191			1739
	6.259	6.068	6.182	6.120	0.651	1741.3					
^{230}U	5.964	5.739	5.875	5.795	0	1756.0	1752.6	0.199		0.260	1752.8
	6.000	5.765	5.907	5.821	0.234	1755.4					
	6.293	6.091	6.213	6.143	0.658	1753.7					
^{232}U	5.994	5.755	5.900	5.810	0	1766.8	1765.7	0.207		0.267	1765.9
	6.033	5.785	5.935	5.840	0.251	1768.2					
	6.364	6.167	6.286	6.218	0.712	1766.8					
^{234}U	6.021	5.767	5.923	5.823	0	1776.4	1778.2	0.215	5.829	0.265	1778.6
	6.065	5.803	5.963	5.858	0.267	1780.3					
	6.415	6.209	6.334	6.260	0.738	1778.2					
^{236}U	6.092	5.819	5.987	5.874	0.276	1791.7	1790.0	0.215	5.843	0.272	1790.4
	6.446	6.230	6.363	6.281	0.744	1789.4					
^{238}U	6.124	5.838	6.015	5.892	0.283	1802.5	1801.2	0.215	5.857	0.272	1801.7
	6.488	6.263	6.402	6.314	0.763	1800.4					

6.50 MeV, respectively. Similarly, the calculated B_f of ^{232}U is 5.65 MeV, which also agree well with the experimental data 5.40 MeV. In some cases, the fission barrier height is $1-2$ MeV lower or higher than the experimental data. The double-humped fission barrier in all these cases are reproduced. Similar type of calculations are also done in Refs. [41–44].

In nuclei like $^{228-230}$Th and $^{228-234}$U, we find three maxima. Among these maxima, two of them are found at normal deformation (spherical and normal prolate), but the third one is situated far away, i.e., at relatively large quadrupole deformation. With a careful inspection, one can also see that one of them (mostly the peak nearer to the spherical region) is not strongly pronounced and can be ignored in certain cases. This third maximum separate the second barrier with a depth of 1 - 2 MeV, responsible for the formation of resonance state, which are observed experimentally[45]. Some of the

TABLE II: Same as Table I, but for Th isotopes.

Nucleus	RMF (NL3)						FRDM		Experiment		
	r_n	r_p	r_{rms}	r_{ch}	β_2	BE (MeV)	BE (MeV)	β_2	r_{ch}	β_2	BE(MeV)
^{216}Th	5.781	5.594	5.704	5.651	0	1673.5	1663.6	0.008			1662.7
	6.034	5.897	5.977	5.951	0.567	1663.8					
^{218}Th	5.812	5.611	5.730	5.667	0	1686.5	1677.2	0.008			1676.7
	6.105	5.959	6.045	6.013	0.616	1678.2					
^{220}Th	5.842	5.631	5.757	5.687	0	1698.1	1690.2	0.030			1690.6
	6.140	5.983	6.076	6.036	0.624	1692.8					
^{222}Th	5.873	5.651	5.784	5.707	0	1709.7	1704.6	0.111		0.151	1704.2
	6.174	6.007	6.107	6.060	0.631	1706.1					
^{224}Th	5.902	5.672	5.81	5.728	0	1721.4	1717.4	0.164		0.173	1717.6
	6.222	6.021	6.142	6.074	0.640	1718.9					
^{226}Th	5.931	5.692	5.837	5.748	0	1733.0	1729.9	0.173		0.225	1730.5
	6.25	6.036	6.166	6.089	0.642	1731.9					
^{228}Th	5.955	5.710	5.859	5.766	0	1743.9	1742.5	0.182	5.748	0.229	1743.0
	5.989	5.729	5.888	5.785	0.227	1744.5					
	6.292	6.065	6.203	6.118	0.661	1743.4					
^{230}Th	5.990	5.727	5.888	5.783	0	1754.2	1754.6	0.198	5.767	0.246	1755.1
	6.026	5.751	5.920	5.807	0.232	1756.0					
	6.315	6.111	6.236	6.163	0.671	1753.1					
^{232}Th	6.060	5.773	5.950	5.828	0.251	1767.0	1766.2	0.207	5.784	0.248	1766.7
	6.240	6.010	6.151	6.063	0.681	1765.0					
^{234}Th	6.093	5.793	5.979	5.848	0.269	1777.5	1777.2	0.215		0.238	1777.6
^{236}Th	6.122	5.812	6.006	5.866	0.272	1787.6	1787.6	0.215			1788.1
^{238}Th	6.152	5.832	6.033	5.887	0.281	1797.5	1797.7	0.224			1797.8
^{240}Th	6.180	5.846	6.057	5.901	0.292	1806.6	1807.2	0.224			

uranium isotopes $^{216-230}$U, the ground states are predicted to be spherical in RMF formalism agreeing with the FRDM results. The other isotopes of the series $^{232-256}$U are found to be prolate ground state matching with the experimental data. Similarly, the thorium nuclei $^{216-226}$Th are spherical in shape and $^{228-264}$Th are prolate ground configuration. In addition to these shapes, we also notice sallow regions in the PES curves of both Th and U isotopes. These fluctuation in the PES curves could be due to the limitation of mean field approximation and one needs a theory beyond mean field to over come such fluctuations. For example, the Generator Coordinate Method or Random Phase Approximation could be some improved formalism to take care of such effects [46]. Beyond the second

hump, we find the PES curve goes down and down, which never ups again. This is the process of the liquid drop gets more and more elongation and reaches to the fission stage. The PES curve, from which it starts downing is marked the scission points which are shown by the black dot in some of the PES curves of Figs. 2 and 3.

D. Evolution of single-particle energy with deformation

In this subsection, we evaluate the neutron and proton single-particle energy levels for some selected Nilssion orbits with different values of deformation parameter β_2 using the

TABLE III: First fission barrier heights B_f (in MeV) of some even-even actinide nuclei from RMF(NL3) calculations compared with FRDM and experimental data [28].

Nucleus	$B_f^{cal.}$	B_f^{FRDM} [28]	$B_f^{exp.}$ [28]
^{228}Th	5.69	7.43	6.50
^{230}Th	5.25	7.57	7.0
^{232}Th	4.85	7.63	6.30
^{234}Th	4.34	7.44	6.65
^{232}U	5.65	6.61	5.40
^{234}U	6.30	6.79	5.80
^{236}U	6.64	6.65	5.75
^{238}U	7.15	4.89	5.90
^{240}U	7.66	5.59	5.80

constraint calculations. The results are given in Figs. 4 and 5, explain the origin of the shape change along the α-decay chains of the thorium and uranium isotopes. The positive parity orbit is the solid line, negative parity orbit is dash line and the dotted line (red colour) indicates the Fermi energy for ^{232}Th and ^{236}U.

FIG. 5: (Color online) Same as Fig. 4, but for ^{236}U nucleus.

tinct shell gap at N=114. In ^{232}Th and ^{236}U, with increasing deformation the opposite parity levels of $2g_{9/2}$ and $1j_{15/2}$ come closer to each other, which are far apart in the spherical solution. This gives rise to the parity doublet phenomena [48–50].

IV. MODE OF DECAYS

In this section, we will discuss about various mode of decays encounter by superheavy nuclei both in the β-stability line as well as away from it. This is important, because the utility of superheavy and mostly the nuclei which are away from stability lines depend very much on their life time. For example, we do not get ^{233}U and ^{239}Pu in nature, because of their short life time, although these two nuclei are extremely useful for energy production. That is why ^{235}U is the most necessary isotope in the uranium series for its thermally fissile nature in the energy production in fission process both for civilian as well as military use. The common mode of instability for such heavy nuclei are spontaneous fission, α-, β- and *cluster*-decays. All these decays depend on the neutron to proton ratio as well as the number of nucleons present in the nucleus.

A. α- and β-decays half-lives

In the previous papers[4, 5], we have analyzed the densities of nuclei in a more detailed manner. From this analysis, we concluded that there is no visible cluster either in the ground or in the excited intrinsic states. The possible clusterizations are the α-like matter at the interior and neutron-rich matter at the exterior region of the normal and neutron-rich superheavy nuclei, respectively. Thus, the possible mode of decays are the α-decay for β-stable nuclei and β^--decay for neutron-rich

FIG. 4: (Color online) Single-particle energy levels for ^{232}Th as a function of quadrupole deformation parameter β_2. The Fermi levels are denoted by thick dotted(red) curve.

For small Z nuclei, the electrostatic repulsion is very weak but at higher value of Z (superheavy nuclei), the electrostatic repulsion is much stronger that the nuclear liquid drop becomes unstable to surface distortion [47] and fission. In such nucleus, the single-particle density is very large and the energy separation is small, which determines the shell stabilizes the unstable Coulomb repulsion. This effect is clear for heavy elements approaching N=126 with the gap between $3p_{1/2}$ and $1i_{11/2}$ of about 2-3 MeV, in the neutron single-particle of ^{236}U and ^{232}Th. In both the figures, the neutron single particle energy level $1i_{13/2}$ lies between $2f_{7/2}$ and $2f_{5/2}$ creating a dis-
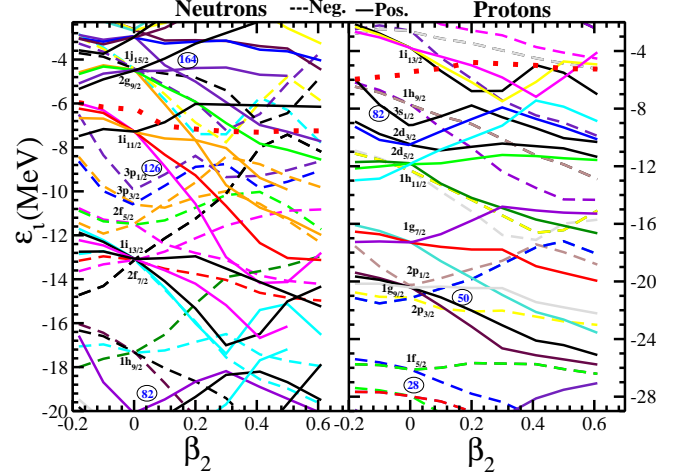
isotopes. To estimate the stability of such nuclei, we have to calculate the α-decay $T_{1/2}(\alpha)$ and the β-decay $T_{1/2}(\beta)$ half-lives times.

1. The Q_α energy and α-decay half-life $T_{1/2}^\alpha$

To calculate the α-decay half-life $T_{1/2}^\alpha$, one has to know the Q_α energies of the nucleus. This can be estimated by knowing the binding energies (BE) of the parents, daughter and binding energy of the α-particle, i.e., the BE of ^{4}He. The binding energies are obtained from experimental data wherever available and from other mass formulae as well as relativistic mean field Lagrangian as we have discussed earlier in this paper [51]. The Q_α energy is evaluated by using the relation:

$$
\begin{aligned}
Q_\alpha(N,Z) &= BE(N,Z) - BE(N-2,Z-2) \\
&\quad - BE(2,2)
\end{aligned}
\tag{13}
$$

Here, $BE(N,Z)$, $BE(N-2,Z-2)$ and $BE(2,2)$ are the binding energies of the parent, daughter and ^{4}He nuclei (BE= 28.296 MeV) with neutron number N and proton number Z.
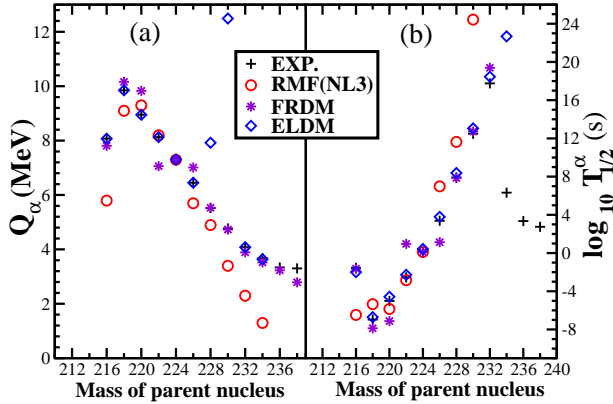

FIG. 6: (Color online) Q_α and half-life time $T_{1/2}^\alpha$ of the α-decay chain for Th isotopes are calculated using RMF, FRMD [28, 29] , ELDM [52] and compared with the experiment [30].

Knowing the $Q_\alpha-$values of nuclei, we roughly estimate the α-decay half-lives $log_{10}T_{1/2}^\alpha(s)$ of various nuclei using the phenomenological formula of Viola and Seaborg [53]:

$$
log_{10}T_{1/2}^\alpha(s) = \frac{(aZ-b)}{\sqrt{Q_\alpha}} - (cZ+d) + h_{log}. \tag{14}
$$

The value of the parameters a, b, c and d are taken from the recent modified parametrizations of Sobiczewski et al. [54], which are $a = 1.66175$; $b = 8.5166$; $c = 0.20228$; $d = 33.9069$. The quantity h_{log} accounts for the hindrances associated with the odd proton and neutron numbers as given by Viola and Seaborg [53], namely
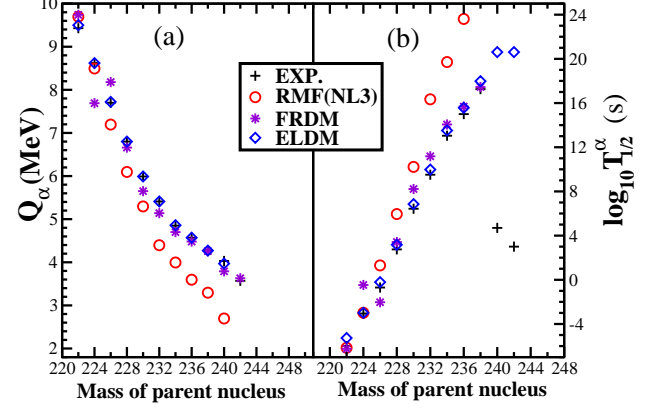

FIG. 7: (Color online) Same as Fig. 6, but for U.

$$
h_{log} = \begin{cases} 0, & \text{Z and N even} \\ 0.772, & \text{Z odd and N even} \\ 1.066, & \text{Z even and N odd} \\ 1.114, & \text{Z and N odd.} \end{cases}
$$

The $Q_\alpha-$values obtained from RMF calculations for Th and U isotopes are shown in Figs. 6 and 7. Our results also compared with other theoretical predictions [29, 52] and experimental data [31]. The agreement of RMF results with others as well as with experiment is pretty well. Although, the agreement in $Q_\alpha-$value is quite good, one has to note that the $T_{1/2}^\alpha(s)$ values may vary a lot, because of the exponential factor in it. That is why it is better to compare $log_{10}T_{1/2}^\alpha(s)$ instead of $T_{1/2}^\alpha(s)$. These values are compared in the right panel of Figs. 6 and 7. We notice, our prediction matches well with other calculations as well as experimental data.

Further, a careful analysis of $log_{10}T_{1/2}^\alpha$ (in seconds) for even-even thorium, the $Q_\alpha-$value decreases with increase of mass number A of parent nucleus. The Q_α energy of Th isotopes given by Duarte et al. [52] deviates a lot, when mass of the parent nucleus reaches to A=230. The corresponding $log_{10}T_{1/2}^\alpha$ increases almost monotonically linearly with an increase of mass number of the same nucleus. The experimental values of $log_{10}T_{1/2}^\alpha$ deviate a lot in the heavy mass region, (with parent nuclei 234-238). Similar situation is found in case of uranium isotopes also which are shown in Fig. 7.

B. β-decay

As we have discussed, the prominent mode of instability of neutron-rich Th and U nuclei is the β-decay, and we have given an estimation of such decay in this subsection. Actually, the β-decay life time should be evaluated in a microscopic level, but in this paper, it is beyond the scope. Here we have used the empirical formula of Fiset and Nix [55], which is defined as:
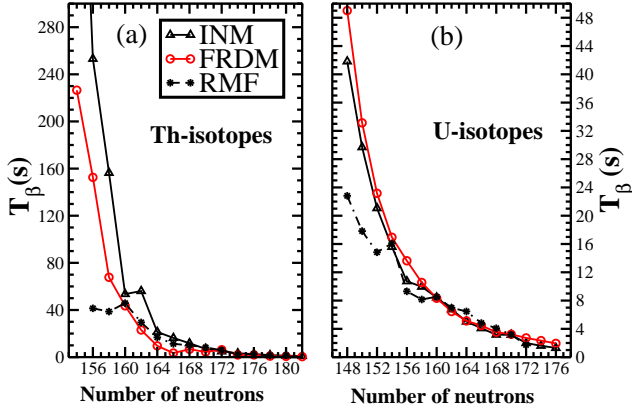
FIG. 8: (Color online) The β-decay half life for Th and U isotopes are calculated using the formula of Fiset and Nix [55] [eq. (24)]. The ground state binding energies are taken from FRDM [29], INM [56] and RMF models.

$$T_\beta = (540 \times 10^{5.0}) \frac{m_e{}^5}{\rho_{d.s.}(W_\beta{}^6 - m_e{}^6)} s. \quad (15)$$

Similar to the α-decay, we evaluate the Q_β-value for Th and U series using the relation $Q_\beta = BE(Z+1,A) - B(Z,A)$ and $W_\beta = Q_\beta + m_e{}^2$. Here, $\rho_{d.s.}$ is the average density of states in the daughter nucleus ($e^{-A/290} \times$ number of states within 1 MeV of ground state). To evaluate the bulk properties, such as binding energy of odd-Z nuclei, we used the Pauli blocking prescription as discussed in Section II. The obtained results are displayed in Fig. 8 for both Th and U isotopes. From the figure, it is clear that for neutron-rich Th and U nuclei, the prominent mode of decay is β-decay. This means, once the neutron-rich thermally fissile isotope is formed by some artificial mean in laboratory or naturally in supernovae explosion, immediately it undergoes β-decay. In our rough estimation, the life time of ^{254}Th and ^{256}U, which are the nuclei of interest has tens of seconds. If this prediction of time period is acceptable, then in nuclear physics scale, is reasonably a good time for further use of the nuclei. It is worthy to mention here that thermally fissile isotopes of Th and U series are with neutron number N=154-172 keeping N=164 in the middle of the island. So, in case of the short life time of ^{254}Th and ^{256}U, one can choose a lighter isotope of the series for practical utility.

C. Limitations of the model

Before drawing the concluding remarks, it is important to mention few points about the limitations of our present approach. When we compare our calculated results with the experimental data, although we get satisfactory results, some time we do not get excellent agreement and the main possible reasons for the discrepancy of RMF with experimental values

are given as:

(1) In RMF formalism we are working in the mean field approximation of the meson field. In this approximation, we are neglecting the vacuum fluctuation, which is an indispensable part of the relativistic formalism. In calculating the nucleonic dynamics, we are neglecting the negative energy solution that means, we are working in the no sea approximation [57]. It is already discussed that the no-sea approximation and quantum fluctuation can improve the results upto a maximum of 20% [58] for very light-nuclei. Therefore, the mean field is not a good approach for the light region of the periodic table. However, for the heavy masses, this mean field approach is quite good and can be used for any practical purpose.

(2) In order to solve the nuclear many body system, here we used the Hartee formalism and neglect Fock term, which corresponds to the exchange correlation.

(3) To take care of the pairing correlation, we have used BCS type pairing approach. This gives good results for the nuclei near the β-stability line, but it fails to incorporate properly the pairing correlation for the nuclei away from the β-stability line and superheavy nuclei [23]. Thus a better approach like Hartree-Fock-Bogoliubov [59, 60] type pairing co-relation is more suitable for the present region.

(4) Parametrization plays an important role in improvising the results. The constants in RMF parametrizations, are determined by fixing the experimental data for few spherical nuclei. We expect that the results may be improved by re-fitting the force parameters for more number of nuclei, including the deformed isotopes.

(5) The basic assumption in the RMF theory is that two nucleons interact with each other through the exchange of various mesons. There is no direct inclusion of 3-body or higher body effects. This effect is taken care partially by including the self-coupling of mesons and in recent relativistic approach various cross-couplings are added because of their importance.

(6) Although, there are various mesons are observed experimentally, few of them are taken into account in the nucleon-nucleon interaction. Contribution of some of them are prohibited due to symmetry reason and many are neglected due to their negligible contributions, because of heavy mass. However, some of them has substantial contribution to the properties of nuclei, specially when the neutron-proton asymmetry is more, such as δ-meson [61, 62].

(7) It is to be noted that the origin of α-decay or *cluster*-decay phenomena are purely quantum mechanical process. Thus the quantum tunneling plays an important role in such decay processes. The deviation of experimental α-decay life time from the calculated results obtained by the empirical formula may not be suitable for such heavy nuclei, which are away from the stability line and more involved quantum me-

chanical treatment is needed for such cases.

V. CONCLUSIONS

In summary, we did a thorough structural study of the recently predicted thermally fissile isotopes of Th and U series in the framework of relativistic mean field theory. Although there are certain limitations of the present approach, the qualitative results will remain unchanged even if the draw-back of the model taken into account. The heavier isotopes of these two nuclei bear various shapes including very large prolate deformation at high excited configurations. The change in single-particle orbits along the line of quadrupole deformation are analyzed and found parity doublet states in some cases.

Using an empirical estimation, we find that the neutron-rich isotopes of these thermally fissile nuclei are predicted to be stable against α- and *cluster*-decays. The spontaneous fission also does not occur, because the presence of large number of neutrons makes the fission barrier broader. However, these nuclei are highly β-unstable. Our calculation predicts that the β-life time is about tens of seconds for ^{254}Th and ^{256}U and this time increases for nuclei with less neutron number, but thermally fissile. This finite life time of these thermally fissile isotopes could be very useful for energy production in nuclear reactor technology. If these neutron-rich nuclei use as nuclear fuel, the reactor will achieve critical condition much faster than the normal nuclear fuel, because of the release of large number of neutrons during the fission process.

[1] L. Satpathy, S. K. Patra and R. K. Choudhury, Pramana J. Phys. **70**, 87 (2008).
[2] P. Arumugam, B. K. Sharma, S. K. Patra and R. K. Gupta, Phys. Rev. C **71**, 064308 (2005).
[3] BirBikram Singh, B. B. Sahu and S. K. Patra, Phys. Rev. C **83**, 064601 (2011).
[4] S. K. Patra, Raj. K. Gupta, B. K. Sharma, P. D. Stevenson and W. Greiner, J. Phys. G. **34**, 2073 (2007).
[5] B. K. Sharma, P. Arumugam, S. K. Patra, P. D. Stevenson, R. K. Gupta and W. Greiner, J. Phys. G. **32**, L1 (2006).
[6] G. R. Satchler and W. G. Love, Phys. Rep. **55**, 183 (1979).
[7] BirBikram Singh, M. Bhuyan, S. K. Patra and Raj. K. Gupta, J. Phys. G. **39**, 025101 (2012).
[8] B. B. Sahu, S. K. Singh, M. Bhuyan, S. K. Biswal and S. K. Patra, Phys. Rev. C **89**, 034614 (2014).
[9] G. A. Lalazissis , J. König and P. Ring, Phys. Rev. C **55**, 540 (1997).
[10] S. K. Patra and C. R. Praharaj, Phys. Rev. C **44**, 2552 (1991).
[11] J. D. Walecka, Ann. Phys. **83**, 491 (1974).
[12] B. D. Serot and J. D. Walecka, Adv. Nucl. Phys. **16**, 1 (1986).
[13] C. J. Horowitz and B. D. Serot, Nucl. Phys. A **368**, 503 (1981).
[14] J. Boguta and A. R. Bodmer, Nucl. Phys. A **292**, 413 (1977).
[15] C. E. Price and G. E. Walker, Phys. Rev. C **36**, 354 (1987).
[16] P. G. Blunden and M. J. Iqbal, Phys. Lett. B **196**, 295 (1987).
[17] P. G. Reinhard, Rep. Prog. Phys. **52**, 439 (1989).
[18] Y. K. Gambhir, P. Ring and A. Thimet, Ann. of Phys. **198**, 132 (1990).
[19] S. K. Patra, Phys. Rev. C **48**, 1449 (1993).
[20] M. A. Preston and R. K. Bhaduri, *Structure of Nucleus, Addison-Wesley Publishing Company*, Ch. 8, page 309 (1982).
[21] D. G. Madland and J. R. Nix, Nucl. Phys. A **476**, 1 (1981).
[22] J. Dechargé and D. Gogny, Phys. Rev. C **21**, 1568 (1980).
[23] S. Karatzikos, A. V. Afanasjev, G. A. Lalazissis and P. Ring, Phys. Lett. B **689**, 72 (2010).
[24] J. R. Stone and P. G. Reinhard, Prog. Part. Nucl. Phys. **58**, 587 (2007).
[25] F. Tondeur, S. Goriely, J. M. Pearson, and M. Onsi, Phys. Rev. C **62**, 024308 (2000).
[26] U. Hofmann and P. Ring, Phys. Lett. B **214**, 307 (1988).
[27] G. A. Lalzissis, D. Vretenar, and P. Ring, Nucl. Phys. A **650**, 133 (1999).
[28] P. Möller, J. R. Nix and K. L. Kratz, At. Data and Nucl. Data Tables **59**, 185 (1995).

[29] P. Möller, J. R. Nix, W. D. Myers and W. J. Swiatecki, At. Data and Nucl. Data Tables **66**, 131 (1997).
[30] http://www.nndc.bnl.gov/nudat2/
[31] I. Angeli and K. P. Marinova, At. Data and Nucl. Data Tables **99**, 69 (2013).
[32] Zhongzhou Ren and Hiroshi Toki, Nucl. Phys. A **689**, 691 (2001).
[33] Zhongzhou Ren, Ding-Han Chen, Fei Tai, H. Y. Zhang, and W. Q. Shen, Phys. Rev. C **67**, 064302 (2003).
[34] Z. Patyk and A. Sobiczewski, Nucl. Phys. A **533**, 132 (1991).
[35] S. Bjφrnholm and J. E. Lynn, Rev. Mod. Phys. **52**, 715 (1980).
[36] S. K. Patra, F. H. Bhat, R. N. Panda, P. Arumugam and R. K. Gupta, Phys. Rev. C **79**, 044303 (2009).
[37] H. Flocard, P. Quentin and D. Vautherin, Phys. Lett. B **46**, 304 (1973).
[38] W. Koepf and P. Ring, Phys. Lett. B **212**, 397 (1988).
[39] J. Fink, V. Blum, P. G. Reinhard, J. A. Maruhn and W. Greiner, Phys. Lett. B **218**, 277 (1989).
[40] D. Hirata, H. Toki, I. Tanihata and P. Ring, Phys. Lett. B **314**, 168 (1993).
[41] J. Meng, H. Toki, S. G. Zhou, S. Q. Zhang, W. H. Long and L. S. Geng, Prog. Part. Nucl. Phys. **57**, 470 (2006).
[42] Bing-Nan Lu, En-Guang Zhao and Shan-Gui Zhou, Phys. Rev. C **85**, 011301(R) (2012).
[43] Bing-Nan Lu, Jie Zhao, En-Guang Zhao and Shan-Gui Zhou, Phys. Rev. C **89**, 014323 (2014).
[44] Jie Zhao, Bing-Nan Lu, Dario Vretenar, En-Guang Zhao and Shan-Gui Zhou, Phys. Rev. C **91**, 014321 (2015).
[45] B. B. Back, H. C. Britt, J. D. Garrett, and O. Hansen, Phys. Rev. Lett. **28**, 1707 (1972); J. Blons, C. Mazur, D. Paya, M. Ribrag, and H. Weigmann, ibid. **41**, 1282 (1978).
[46] D. M. Brink and A. Weiguny, Phys. Lett. B **26**, 497 (1968).
[47] Myers and W. D. Swiatecki, Nucl. Phys. **81**, 1 (1966).
[48] S. K. Singh, C. R. Praharaj and S. K. Patra, Cen. Eur. J. Phys. **12**, 42 (2014).
[49] Bharat Kumar, S. K. Singh and S. K. Patra, Int. J. Mod. Phys. **24**, 1550017 (2015).
[50] P. G. Thirolf and D. Habs, Prog. Part. Nucl. Phys. **49**, 325 (2002).
[51] S. K. Patra and C. R. Praharaj, J. Phys. G **23**, 939 (1997).
[52] S. B. Duarte, O. A. P. Tavares, F. Guzman and A. Dimarco, At. Data and and Nucl. Data Table **80**, 235 (2009).
[53] V. E. Viola Jr. and G. T. Seaborg, J. Inorg. Nucl. Chem. **28**, 741

(1966).

[54] A. Sobiczewski, Z. Patyk and S. C. Cwiok, Phys. Lett. **224**, 1 (1989).

[55] E. O. Fiset and J. R. Nix, Nucl. Phys. A **193**, 647 (1972).

[56] R. C. Nayak and L. Satpathy, At. Data and Nucl. Data Tables **73**, 213 (1999).

[57] P. G. Reinhard, M. Rufa, J. Maruhn, W. Greiner and J. Friedrich, Z. Phys. A **323**, 13 (1986).

[58] Z. Y. Zhu, H. J. Mang and P. Ring, Phys. Lett. B **254**, 325

(1991).

[59] P. Ring and P. Schuck, The Nuclear Many-Body Problem, Springer-Verlag, Berlin, 1980.

[60] P. Ring , Prog. Part. Nucl. Phys. **37**, 193 (1996).

[61] S. Kubis and M. Kutschera, Phys. Lett. B **399**, 191 (1997).

[62] S. K. Singh, S. K. Biswal, M. Bhuyan, and S. K. Patra, Phys. Rev. C **89**, 044001 (2014).